Arab J Geosci (2016) 9: 682
DOI 10.1007/s12517-016-2715-0

ORIGINAL PAPER

Geomorphological features and weathering of the Southern Submassif of the Menderes Massif (SW Turkey)

Murat Gül[1] · **Göksu Uslular**[1]

Received: 10 December 2015 / Accepted: 12 October 2016 / Published online: 21 October 2016

Abstract The Southern Submassif crops out in the SW of Turkey. This submassif consists of mostly large feldspar-bearing orthogneisses and to a lesser extent tourmaline-orthoclase-plagioclase-, quartz-, muscovite-, and biotite-bearing leucogranites. The orthogneiss forms domed bald hills. The leucogranites crop out (approximately 2 km^2) in the southeastern lowland of the hill. Those units show various geomorphological features that are typically reported in granitoids. Many studies about the Menderes Massif are related with petrography and metamorphic history. The geomorphological features are not taken into consideration. Field observation, thin section analysis, joint set-foliation measurements, and Schmidt Hammer value determination were done in this study. The pillar structures (castellated and domed types) are among larger structures observed on flanks of the domed bald hill. Geomorphological features such as weathering pits, tafoni, honeycomb structures, polygonal cracks, flared slopes, exfoliation, and boulders are observed. The metamorphism causes mineral alignments that affect the strength of the rock. The studied rocks have high strength in perpendicular direction to foliation. The complex tectonic history caused developments of several joint sets. Differences in mineral strength (e.g., high in quartz, low in biotite and feldspar) increase weathering effect. Underground water percolation through the fractures weakens the rock and causes subsurface weathering. After exhumation, disintegrated materials are stripped off, and then flared slopes, polygonal cracks, and pillar structures are exposed. Surface weathering by wind and water increases the weathering effects and gives rise to a formation of rounded rock edges called spheroidal weathering. Contrary to other granitoid areas, the metamorphism promotes the formation of geomorphological features in the study area.

Keywords Pillar structure · Weathering pit · Orthogneiss · Leucogranite · Southern Submassif of Menderes Massif · SW Turkey

✉ Murat Gül
muratgul@mu.edu.tr

[1] Department of Geological Engineering, Muğla Sıtkı Koçman University, 48000 Kötekli, Muğla, Turkey

Introduction

Geological factors control the geomorphology of the terrains (Migoń and Vieira 2014). Especially, lithological properties of rocks led to the formation of different types and various sizes of landforms. For example, weathering of granitoids may form peculiar landforms owing to chemical and physical processes (Twidale 1986; Migoń 2006). Inselbergs, domes, bornhardts, and tors are significant topographical rises in plain areas, and major geomorphological features are observed in granitoids from different countries (Twidale 1986, 1995; Migoń 2006; Twidale and Bourne 2008). Weathering pits, tafoni, honeycomb weathering, polygonal cracks, spheroidal weathering, flared slopes, and blocks are the examples of other geomorphological structures identified in granitoid rocks (Twidale 1986, 1995; Migoń 2006; Twidale and Bourne 2008). Those structures can also be reported in different rocks (e.g., sandstone, and volcanic rocks) (Campbell and Twidale 1995) and are identified in the southern Submassif of the Menderes Massif in SW Turkey. Some of them present a good scene for sightseeing, trekking, and geopark tourism.

Type and ratio of weathering are mainly controlled by lithological properties, mineralogical compositions (Tuğrul and Zarif 1999); climatic conditions (Campbell and Twidale

1995; Twidale 1997); surface water, underground water, and structural properties (Migoń 2004a, b; Vidal Romani and Twidale 2010); hardness (Černa and Engel 2011); and textural properties and time (Twidale 1986; Migoń 2006). Some properties have great importance in the weathering of granitoids, such as denudation history (Erginal and Ertek 2008), subsurface weathering (Roqué et al. 2013), and magma emplacement (Twidale 1986; Migoń 1996, 2006). The weathering factors are variable depending on the geological history of the lithological unit and latitudes of the exposed rocks. However, metamorphism effects were not documented and discussed in detail within these studies. Moreover, the studies about granites in Turkey have mainly focused on their engineering properties (Tuğrul and Zarif 1999; Ceryan et al. 2008; Dağdelenler et al. 2011; Kilic et al. 2014), whereas the studies about their geomorphological features are limited (Erginal and Ertek 2008).

Both sides of the road among the Yatağan and Çine towns in SW Turkey contain peculiar geomorphological features (Fig. 1). This region has been considered as a geopark for a long time, because of two ancient cities, namely, Stratonikeia and Lagina, and those geomorphological features. The geopark was thought as an alternative tourism for Muğla Province, which is one of the most important summer tourism centers of Turkey. The Southern Submassif is part of the Menderes Massif (Figs. 1 and 2). Leucogranites and orthogneisses have been delineated and mapped under Southern Submassif in this region. Many studies, summarized in the regional geological setting section, were related to lithological properties, metamorphism history, and geological evolution of those units. The leucogranite and orthogneiss show some geomorphological features, which are reported widely in granitoids (Goudie 2004; Migoń 2006) and other rocks (Campbell and Twidale 1995). None of the studies on Menderes Massif has worked on those geomorphological features. Tafoni, polygonal cracks, flared slope, and several other geomorphological features can be identified in this region. Metamorphism history and related characteristics of the Southern Submassif are the diagnostic features compared to the other regions that have similar geomorphological features. The main aims of this study are to document the types and distributions of geomorphological features of the Southern Submassif and to discuss the metamorphism effects, such as foliation and mineral differentiation on the weathering and the evolution of the geomorphological features.

Material and method

This study is performed in the SE region of the Southern Submassif (Figs. 1 and 2). The geomorphological features of leucogranite and orthogneiss have been documented, noted, and photographed. Their dominant distributions and dimensions have been recorded. Metamorphic properties, mineral content, and alignment of them were researched. Foliations of the orthogneiss were measured. Thin sections of representative samples were analyzed by using polarizing microscopes in the general geology laboratory of Muğla Sıtkı Kocman University. Discontinuities of leucogranite and orthogneiss were measured, and dominant sets have been evaluated by using DIPS software. In order to determine the strength of the leucogranite and orthogneiss, the L-type Schmidt hammer has been used during the field studies. The hammer was applied in parallel and perpendicular directions to foliation.

Regional geology

The Menderes Massif (MM) is the largest (>40,000 km^2) metamorphic core complex exposed in the Alpine orogenic belt (Fig. 1; Şengör et al. 1984; Bozkurt et al. 1995; Bozkurt and Oberhansli 2001; Whitney and Bozkurt 2002). The Southern Submassif is the southern part of the Menderes Massif. The central part of the Southern Submassif includes 700–750-m-high hills. The eastern and southern sides of these hills are cut by valleys (Fig. 2). The core of the Southern Submassif contains Upper Proterozoic metasediments, mica schist, orthogneiss, metagabbros, and metanorite intrusions (Figs. 1 and 2; Candan et al. 2001; Dora et al. 2001). The Massif is overlain by cover units including Paleozoic-Lower Tertiary platform carbonates, marl, clayey limestone, and marble (Figs. 1 and 2; Okay 2001; Özer et al. 2001).

A few studies have been performed on the detailed geology of the studied region (Mineral Research Institute-MTA; Bozkurt 2004; Koralay et al. 2012; Bozkurt et al. 2015). Precambrian migmatite, gneiss, augen gneiss, metagranitoid, Paleozoic augen gneiss, phyllite, schist, marble, and quartzite in the southern region were mapped in 1/25,000-scaled geologic maps prepared by MTA (Figs. 2 and 3). Bozkurt (2004) identified leucogranite including K-feldspar, plagioclase, quartz, muscovite, biotite, tourmaline, zircon, rutile, monazite, and opaque minerals around the Hacıaliler district (Fig. 2). Blastomylonitic orthogneisses with muscovite, biotite, quartz band and flattened feldspar (augen) are exposed in northern part of the metagranite (Bozkurt 2004). Semipelitic schist, marble lenses, psammitic schist crop out in southern part of the leucogranites (Bozkurt 2004). Bozkurt et al. (2015) reported that the leucogranite (late Middle Eocene) intruded to the orthogneisses and cover units of the Southern Submassif. However, Koralay et al. (2012) classified those rocks in and around the Hacıaliler district as leuco-tourmaline orthogneiss and biotite orthogneiss.

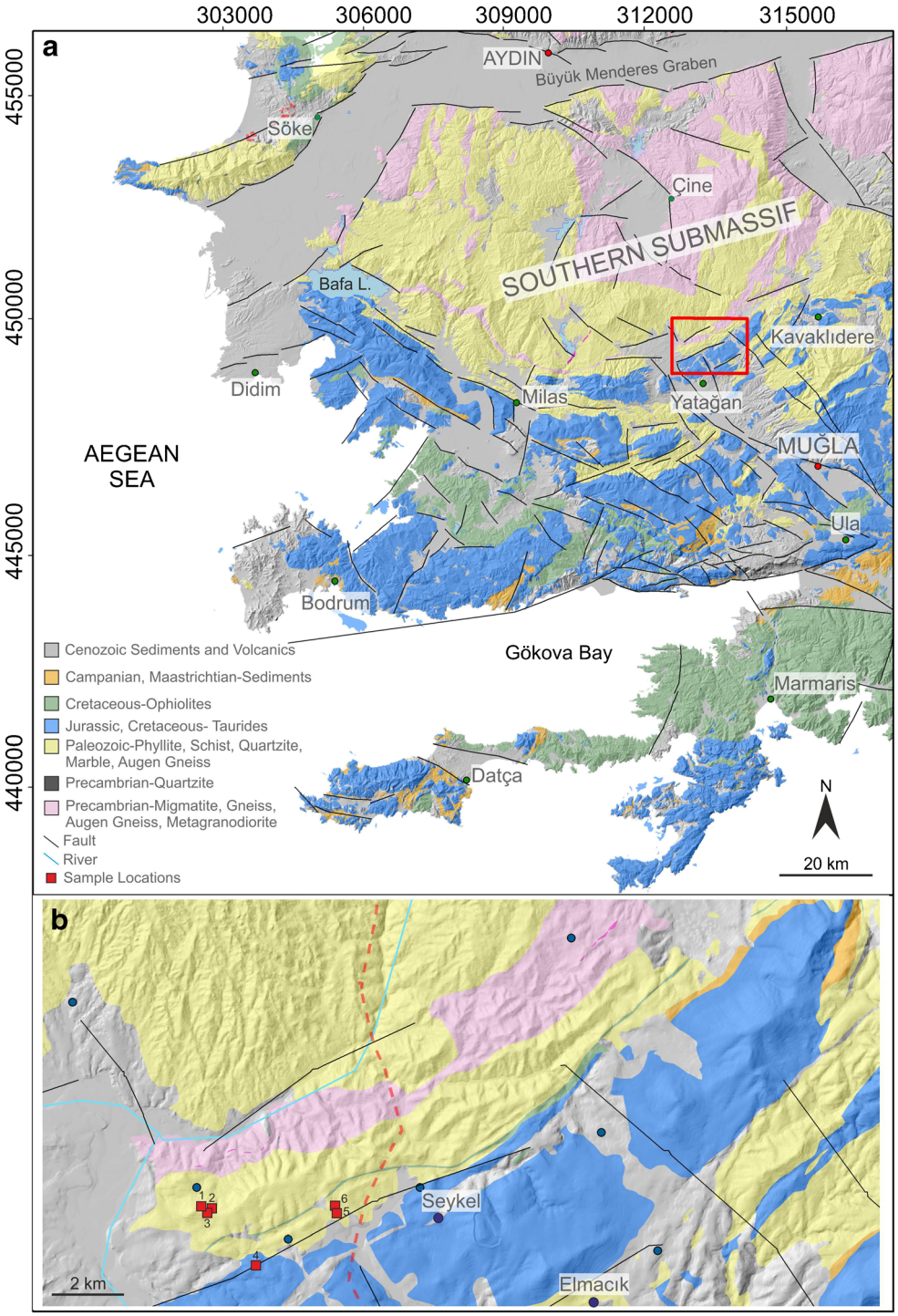

Fig. 1 Location map of the study area. **a** General geological map and DEM view of the Southern Submassif and surrounding region (after Okay 2001; Whitney and Bozkurt 2002). *Red rectangular area* shows the location of the view in **b**. **b** Detailed DEM view of the study area

These units intruded to southern garnet-mica schist and biotite-albite schist (Koralay et al. 2012).

Metamorphism and tectonic history of southern Submassif

This massif was affected by two main metamorphisms that are regional HT/MP Barrovian-type in Eocene and subsequent greenschist retrograde metamorphism (Şengör and Yılmaz 1981; Şengör et al. 1984; Bozkurt and Satır 2000; Bozkurt and Oberhansli 2001; Rimmele et al. 2003; Bozkurt 2004). The southward transport of Lycian nappes (ophiolites, accretionary prisms, volcanosedimantary units, and Carboniferous-Permian-Upper Cretaceous sedimentary rocks) over the Menderes Massif has caused regional metamorphism (Şenel 1997;

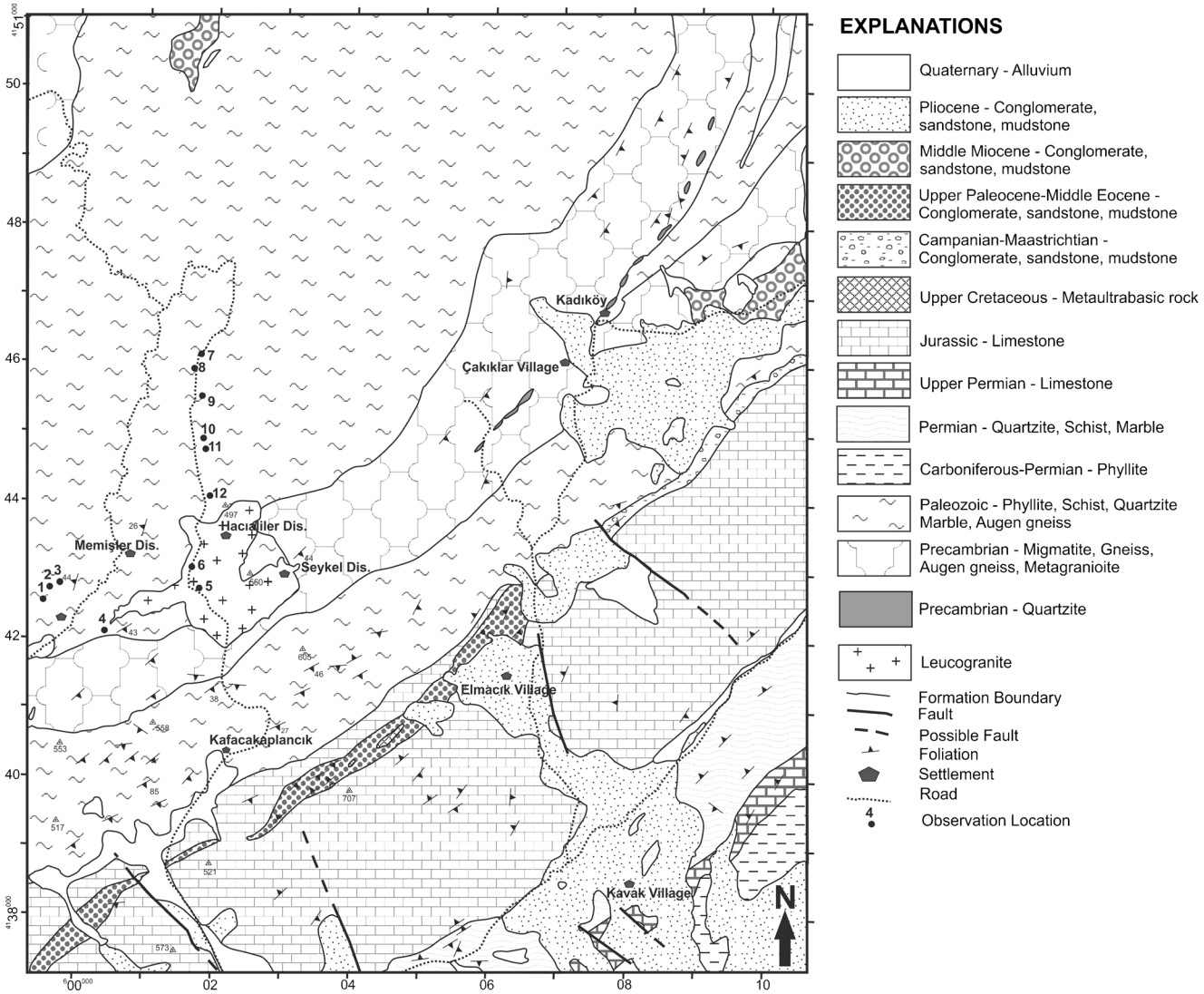

Fig. 2 General geological map of the study area (simplified and modified from MTA map). The leucogranite boundary is obtained from Bozkurt (2004)

Robertson 2000; Bozkurt 2004). After the emplacement of Lycian Nappes to the south of the Southern Submassif, the E–W-trending Kale–Tavas Basin (ancestor of Gökova Graben in Fig. 1) was developed in Oligocene (Görür et al. 1995; Gürer and Yılmaz 2002). Later, NNW–SSE-directed Milas-Ören and Yatağan grabens were subjected to extensional periods in SW Anatolia during the Early–Middle Miocene (Gürer and Yılmaz 2002). The exhumation of the Southern Submassif led to an E–W-trending horst development in Late Miocene (Gürer and Yılmaz 2002) or Oligo-Miocene (Bozkurt 2004; Koralay et al. 2012). Bozkurt et al. (2015) reported the exhumation age of the massif as earliest Miocene based on the unconformable cover sediments. Then, recently active E–W Gökova Graben (Gökova Bay) cuts older units after Late Pliocene (Fig. 1; Görür et al. 1995; Gürer and Yılmaz 2002).

Gemorphological features, weathering profiles, and Grus development

The northern part of the study area includes a domed bald hill and high mountains (250–300 m higher from surroundings, e.g., Gökbel mountain) formed by orthogneiss (Fig. 1). The eastern and southern slopes of it rapidly decrease (Figs. 1, 3, and 4). The slope of the hill contains pillar structures (Figs. 3, 4, and 5). Moreover, other geomorphological features such as boulder, blocks, weathering pits, tafoni, honeycomb weatherings, and polygonal cracks are observed in the leucogranite and orthogneiss outcrops (Figs. 5 and 6). Table 1 summarizes properties and location of those geomorphological features.

Pillar structures are relatively bigger geomorphological features in the study area (Table 1; Figs. 3, 4, and 5).

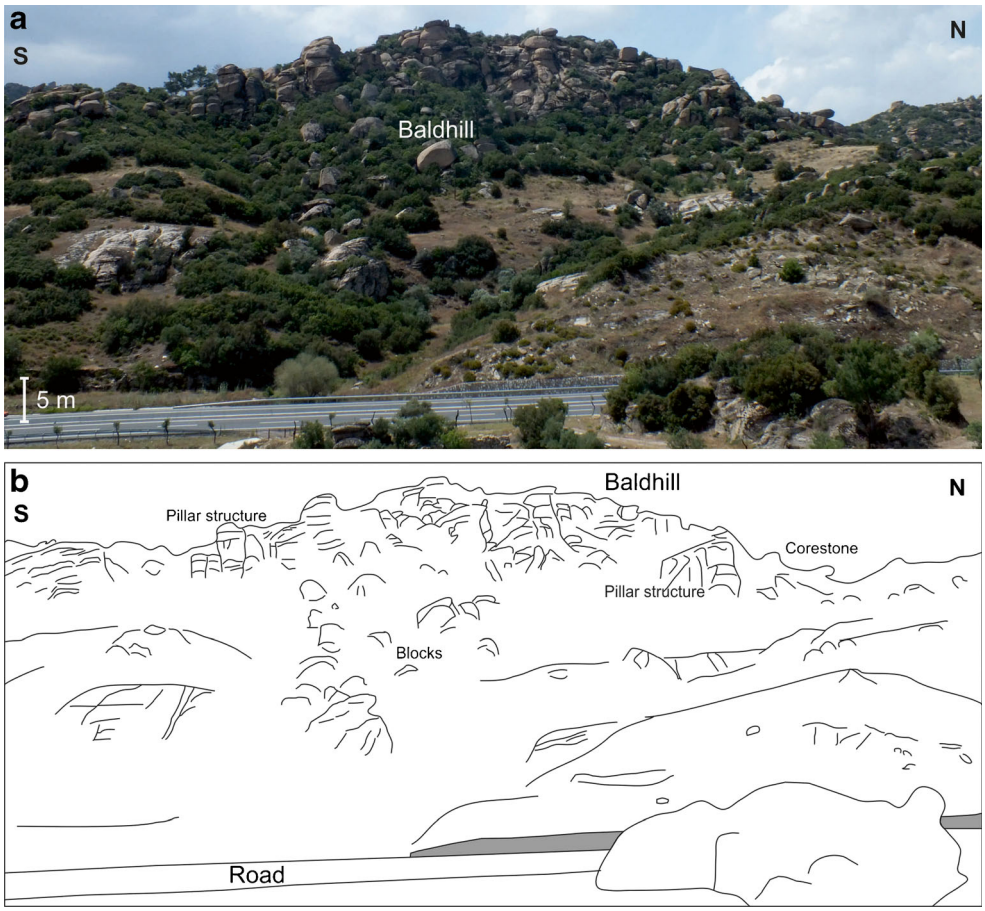

Fig. 3 **a** The orthogneisses form a bald hill north of the Memişler village. **b** *Sketch diagram* of the bald hill containing several pillar structures, corestones, and blocks. Some places have a rocky view, while some places are covered by thin regolith

Crossing of joints, subsequent water weathering followed by cracks, and stripping of disintegrated and decomposed products control their shape, size, and location. Dome-topped pillar structures are smaller than the flat-topped structures. Cracks, which cut the pillar structures, point out the younger structures that developed after weathering. Initially, flat-topped castellated-type pillar structures have been developed, and subsequent spheroidal weathering (possibly surface weathering) led to the development of dome-topped pillar structures.

Weathering pits are depression on the upper surface of the host rock (Table 1; Fig. 6a). These weathering pits like small channels are generally extended parallel to the foliation planes and carry surface water toward edges of rocks (Fig. 6e). They are rarely found at the bottom surface of rocks. Recent water traces have been observed in both upper and bottom surfaces of rocks.

Polygonal cracks are rectangular–pentagonal–hexagonal attached cracks, found on the sidewall of rocks in different sizes (Table 1; Figs. 5a and 6b). Their distributions are random in the study area, and only a few rock surfaces show these features.

Tafoni (tafone in singular) is the most common cavernous weathering type in the study area (Table 1; Figs. 5b and 6c–f). Their size and shape are highly variable (Table 1). Spheroidal weathering is observed at the top of it. Flared slopes are developed in the entrance of tafoni. Water traces and honeycomb weatherings have been found within the tafoni (Fig. 6d). The entrance of the tafoni is generally parallel to the mineral alignment and foliation. After the narrow entrance, tafoni are enlarged inside the upper layer.

Alveoli-honeycomb features are another cavernous but small features. They are developed inside the tafoni as several small chambers (Table 1; Fig. 6d). Water traces are also found in those small chambers.

The boulders and blocks can be found as attached to the host rock and detached blocks (Table 1; Figs. 6f, g). Crossing of joints and stripping of weathered parts led to the formation of attached blocks of various sizes on orthogneisses and leucogranites. Sometimes, blocks are detached from the rock body and transported downdip. Spheroidal weathering is observed on the upper surface of boulders and blocks. Weathering pit rarely causes wavy upper surfaces (Fig. 6g). Red color weathering is observed at the bottom of blocks due to weathering of iron-rich minerals. Generally, flared slopes are found at the lower edge of attached blocks (corestone; Fig. 6g).

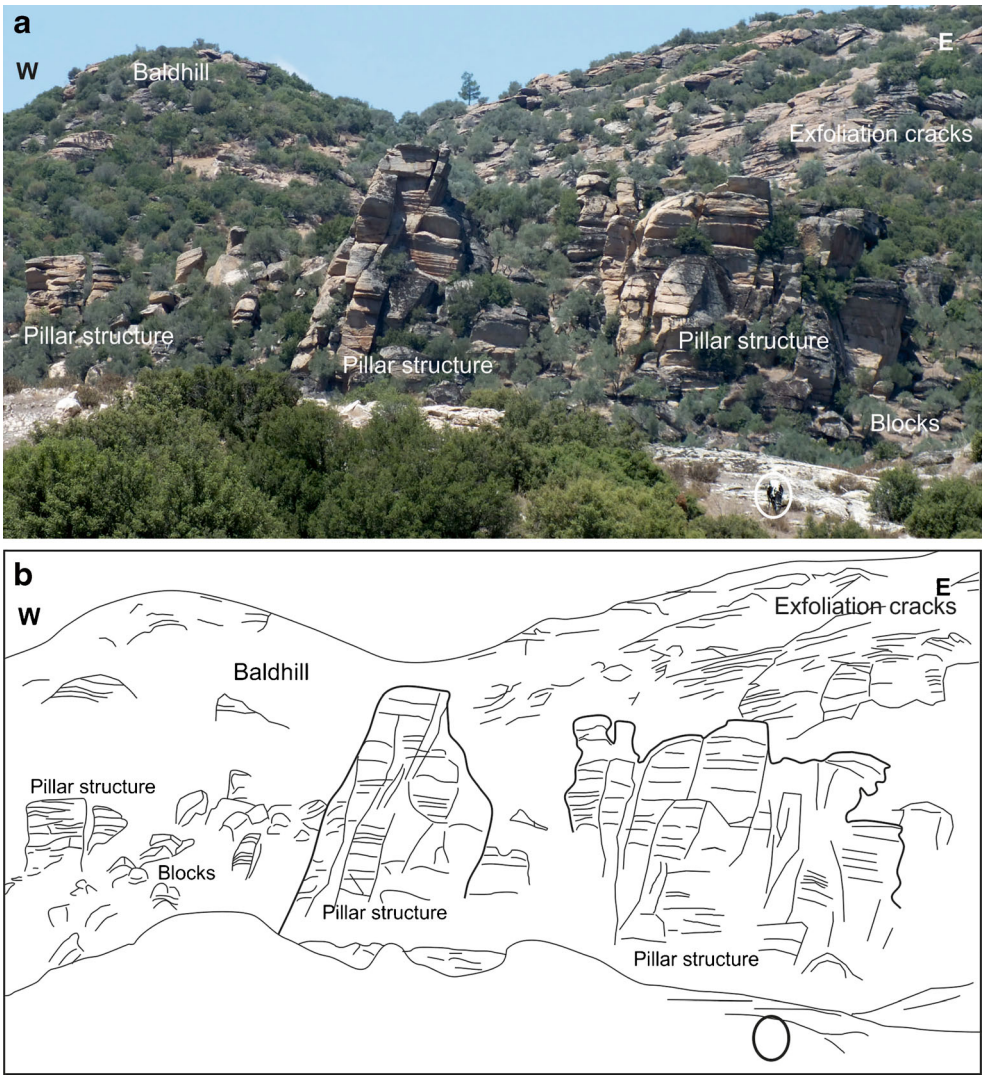

Fig. 4 **a** The orthogneisses form a bald hill southwest of the Memişler village (*cow* in *circle* for scale). **b** *Sketch diagram* of the bald hill. The skirt of the bald hill contains several pillar structures. Each pillar structure is fractured with NS- and EW-directed discontinuity sets. EW-directed exfoliation cracks have also affected these rocks. The crossing of joint sets forms several block–corestone formation

Sometimes, block separation led to the formation of woolsack (Fig. 6g).

The exfoliation cracks, sheeting (onion skin weathering), or pseudobedding are well observed in the orthogneiss than in

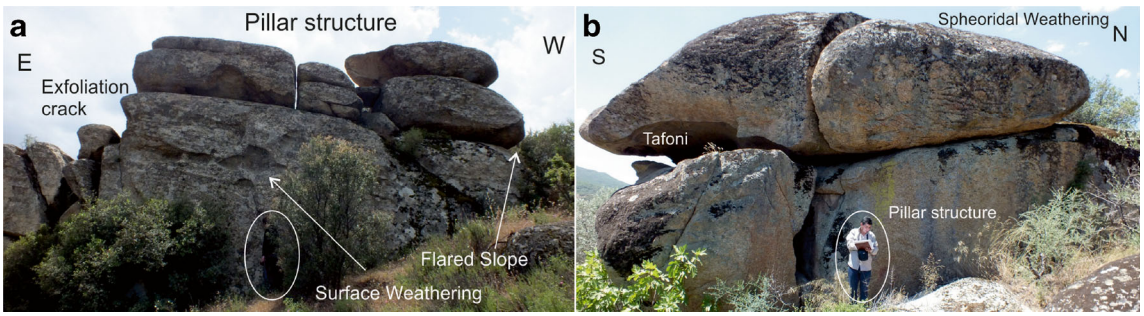

Fig. 5 **a** The pillar structure in orthogneiss (north of Hacıaliler District) is formed by the splitting of rocks along the fractures. Some large rock surface contains surface weathering and polygonal cracking. Some fractures (possibly younger structure) cut the spheroidal weathering (*man* in *circle* for scale: 1.75 m). **b** The pillar structure in leucogranite (south of Hacıaliler District) forms a dome-shaped ridge. The upper parts are sharpened as a result of the spheroidal weathering. Some fractures cut the spheroidal weathering. The tafoni is observed at the top of the pillar. Exfoliation crack is not observed in this type of structure (*man* in *circle* for scale, 1.75 m)

Fig. 6 Field view of the minor geomorphological structures that can be observed both in leucogranites and orthogneiss. **a** The weathering pit is formed as a result of the surface water flowing and selective erosion with various scales (in orthogneiss, SW Memişler village). The water flowing can create depressions with varying scales (hammer in circle for scale, 33 cm). **b** The polygonal crack or surface weathering is formed on the surface of boulder block (in orthogneiss, SW Memişler village; *hammer* in *circle* for scale, 33 cm). **c** Some blocks at the top of the rock contain tafoni with honeycomb weathering (in orthogneiss, N Hacıaliler District). **d** The close inside view of the tafoni includes honeycomb weathering (*hammer* in *circle* for scale, 33 cm). **e** A meter-scaled tafone includes honeycomb weathering and water trace. Two small depressions are observed at the left of the tafoni (in orthogneiss, N Hacıaliler District; *hammer* in *circle* for scale, 33 cm). **f** The selective weathering, tafone formation, and dome shape of the block can lead to the different view of the mushroom rock or corestone. A two to three-meter-scaled spoon-like mushroom rock is formed as a result of the breaking of the dome rock including tafoni (in orthogneiss, N Hacıaliler District). **g** Different types of geomorphological features can be observed in the same location. Fractures, exfoliation orientations, water, and subsurface weathering effect led to the formation of weathering pit, corestone, spheoridal weathering, and woolsack developments (in orthogneiss, N Hacıaliler District). **h** The surface weathering along the exfoliation or cracks led to the formation of spheoridal weathering and flared slope. The size of the flared slope can reach to a maximum of 2 m in height and 2.5 and 3 m in depth (in orthogneiss, N Hacıaliler District; *man* for scale, 1.75 m)

Table 1 Geomorphological features, weathering profiles, and grus development in the Southern Submassif of Menderes Massif

Geomorphological features	Size	Distributions	Properties	Interpretation
Dome hill–bald hill	H: 250–300 m from surroundings, E: 750 m , L: 10 km in EW direction, W: 4–5 km in NS direction.	NNW part of the study area	It is formed in the highest parts of the study area. Other small-scale geomorphological features are located at the flanks of hills (Figs. 3 and 4).	Exhumation of the southern submassif of the Menderes Massif (Bozkurt 2004; Koralay et al. 2012; Bozkurt et al. 2015) and later erosion led to the formation of this dome-topped hill.
Pillar structures	H: <50 m, d: 10–100 m	They crop out in the SSE part of the dome–bald hill	Two different pillar structures have been defined; castellated pillars (Figs. 3, 4, and 5) and dome-topped pillars (Fig. 5). The castellated types are heavily fractured with flat-topped types and are dominantly found in orthogneisses. The other type is a dome-topped pillar.	The pillar structures are formed due to differential weathering of dry rock at the surface and wet rocks in deeper parts (Campbell and Twidale 1995). The properties of subsurface weathering are not clearly observed in the study area. However, crossing of N–S- and E–W-oriented main structures and exfoliation joints led to fracturing of host rocks. After removing weathered and disintegrated parts, relatively stronger and more resistant parts form castellated pillar structures at the beginning. Later, possibly surface weathering smoothens the sharp corners of the upper part of the rocks and led to the formation of a dome-topped pillar structure.
Weathering pits	D: 10–30 cm, L: 40 cm–2 m, and W: 50 cm	They are observed on the slightly inclined upper surface of large blocks of both orthogneiss and leucogranite. It is rarely found at the bottom of the rock surface.	They are elongated hollows with a channelized view on the upper surface of host rocks (Fig. 6a). The closed, oval parts of weathering pits are located at the slightly higher part of the upper surface of blocks, then inclined toward the edge of blocks which are open ended. Some weathering pits carry evaporation traces of surface water. Weathering pits at the bottom of the rock surfaces include recent surface water traces, which are leaked from the side wall of the blocks.	Weathering pits are depression parts developed above the horizontal and low-inclined rock surfaces and can form in different climatic conditions as a result of the chemical dissolutions (e.g., hydration), the mechanic effects of salt and ice, and biochemical weatherings (Twidale and Bourne 2003, 2008). Those types of features are also called gnammas (Domínguez-Villar and Jennings 2008). Water starts to weather the surface of rocks depending on the mineralogical weakness and/or structural weakness, then weathering is continued along the inclination. Leaking of surface water from the side wall passes to the subsurface of rocks and forms the weathering pits.
Polygonal cracks	H: 10–50 cm, W: 10–100 cm, and D: 2–10 cm	Randomly distributed on side walls of large blocks of both orthogneiss and leucogranite	They are rectangular,pentagonal and hexagonal in shape, and rarely irregular shape on the side wall (Figs.5a and 6b). Long edges of cracks are generally parallel to the foliation or mineral alignment. Some cracks are cut by discontinuities.	They start to be formed as a result of subsurface weathering (Twidale and Bourne 1975; Migoń 2006). The underground water follows the discontinuities, then they are dispersed along the side wall via mineral alignment. The surficial weathering of rocks led to the formation of polygonal cracks.
Tafoni-Tafone	H: 50 cm–3 m, D: 30 cm–4 m, and W: 50 cm–3 m. T: 10–50 cm	They are found in both orthogneiss and leucogranite.	Tafoni are mainly found within the dome-shaped blocks with flared slopes and have spheroidal and elliptical shapes (Figs. 5b and 6c–f). They are generally found as caves with a single entrance, but sometimes open in both ends. Water traces and honeycomb weathering have been found within the tafoni (Fig. 6d). Spoon-like morphological appearances are formed with tafoni.	Tafoni (tafone in singular) are the most common types of cavernous weathering features that have spheroidal and elliptical shapes and a concave inner wall with diameter and depth up to several meters (Twidale and Bourne 1975; Campbell 1999; Turkington and Phillips 2004; Strini et al. 2008; Twidale and Bourne 2008). Some tafoni are found with smaller subsurface weathering pits including water traces. Moreover, their entrance

Table 1 (continued)

Geomorphological features	Size	Distributions	Properties	Interpretation
				with flared slopes are parallel to the mineral alignment. After entrance, they are enlarged to the inside of the rocks. Recent view of tafoni; water follows the discontinuities, then it decomposes the rock depending on the mineral weakness along mineral alignments (quartz is hard and resistant, feldspar or other minerals are less resistant) and possible structural features. When the decomposing starts, it is enlarged into the rock.
Alveoli-honeycomb features	W: 10–20 cm, d: up to 10 cm	These small cavernous features are found in tafoni-tafone.	These features include water traces that are carved inside the tafoni more than the surrounding parts (Fig. 6d).	Alveoli-honeycomb features are closely developed by small cavities within the rock caves and are formed in arid climatic conditions and coastal areas. Each chamber within these structures is separated by a thin wall (Twidale and Bourne 2008). The water activities inside the tafone-tafoni led to the formation of these small cavernous structures.
Boulders, blocks	d: 1–5 m	Attached blocks are found on top of orthogneiss and leucogranite; detached blocks are randomly distributed at the flanks of the domed orthogneiss hill.	Attached blocks to the main rock body are called as mushroom rocks and corestones. A joint set can be viewed in all parts of the blocks. Boulders are formed as a result of the complete separation of blocks from the main rock mass, then they are transported in a downdip direction and randomly distributed. Moreover, a flared slope is observed at the bottom part, spheroidal weathering on the upper surface, weathering pit with wavy surface on the upper surface, and rarely woolsack, clefts with boulders (Figs. 6f, g). Red color weathering is observed at the bottom of corestones due to weathering of iron-rich minerals. Some block splitting indicates the effects of tectonic stresses after the spheroidal weathering.	The corestones and boulders are formed as a result of chemical and mechanical weathering of various rock types (Migoń 2006; Turkington 2004a). The formation of corestones is controlled by the climate, lithology, fracture, and two-stage weathering (subsurface weathering andstripping of regolith) (Campbell and Twidale 1995; Twidale 2002). The crossing of the joints led to the formation of blocks. Flared slope and spheoridal weathering are formed as a result of weathering of a sharp corner of the blocks. Some blocks preserve their in situ position (attached blocks); hovewer, some of them are completely separated from the main rock mass (detached blocks) and are transported in a downdip direction. Some discontinuities are cut by spheroidal weathering blocks; they preserve their sharp corner. Thus, they may indicate the subsurface weathering. The rock is weathered in the subsurface, then after the exhumation, weathered materials are stripped off, and some blocks move downdip.
Exfoliation cracks	T: up to 10 cm at the upper part of orthogneiss, T: 3–5 cm at the upper part of leucogranite.	They can be observed at nearly every part of the study area.	They are well observed in orthogneiss than in leucogranite. The exfoliation cracks are parallel to foliation planes of orthogneiss and mineral alignment of leucogranite (Figs. 4 and 5a).	The exfoliation cracks, sheeting (onion skin weathering), or pseudobedding occur depending on the removing of external compression by exhumation and expansive stress (Vidal Romani and Twidale 2010). Exhumation of both orthogneiss and leucogranite led to the development of the exfoliation cracks in the study area.
Spheroidal weathering	Their sizes are variable depending on the weathered mass.	They can be observed at nearly every part of the study area.	Upper surface of blocks and pillar structures are well-rounded due to this weathering (Figs. 5b and 6g, h). Some of them are cut by younger fractures.	Spheroidal weathering is rounded along the fractured blocks and led to the separation of concentric layers on the outer surface of rocks (Nicholson 2004).

Table 1 (continued)

Geomorphological features	Size	Distributions	Properties	Interpretation
Flared slopes	Their sizes are variable. The maximum one has 1 to 1.5 m height and extending 3 m to the rock interior.	They can be observed at nearly every part of the study area.	They are mainly parallel to main discontinuities, mineral alignment of leucogranites, and foliation of orthogneiss (Fig. 6h).	Flared slopes are concave features developed at the base of pillar structures and corestones (Twidale and Bourne 1975, 1998; Migoń 2006). They are indicators of subsurface weathering (Twidale and Bourne 1998, 2008). After development of subsurface weathering of orthogneiss and leucogranite, they are exhumed. The weathering parts are removed downdip. Younger deformational activities, climatic condition, and weathering are buried due to previous geomorphological features such as flared slope, spheoridal weathering, etc.
Weathering profiles	H: 15–20 m, L: 150 m	The thickest weathering profiles are observed only in quartz quarry in orthogneiss. Other profiles are observed along the road cut.	They are observed along the road cut in the orthogneiss (Fig. 7a). The water infiltration increases the weathering effect along the discontinuity surfaces.	The deep weathering profiles include I to VI grades (Thomas 2004). Some of them cannot be observed due to transportation of blocks and stripping of regoliths related to inclination of the slope (Thomas 2004). Deep weathering profiles with various thicknesses are only observed in a few locality along the road cut. The rest of the rocky exposures do not include any product of deep weathering profile. They may stripp off and be transported in a downdip direction. Weathering factors control the thickness of the profile.
Grus	T: 1–1.5 m	It is mainly filled in the valley within the foothills.	The grus contains white-colored and mostly quartz-bearing sediments (Fig. 7b). The boundary between grus and flared slopes is sharp.	Grus is weathered sediment accumulated in front of granitic blocks (Migoń 2006). It is evolved after subsurface weathering (Twidale and Bourne 1998, 2008). Surface and subsurface weathering of orthogneiss and leucogranite led to the formation of complete disintegration. These grains are transported in a downdip direction and accumulated inside the valley.

D depth, *H* height, *E* elevation, *L* length, *W* width, *d* diameter, *T* thickness

the leucogranite. The exfoliation cracks of orthogneiss are parallel to foliation planes (Table 1; Figs. 4 and 5a). They are parallel to mineral alignment in leucogranite.

Spheroidal weathering is responsible for the roundness of boulders, blocks, and upper surfaces of pillar structures (Table 1; Figs. 5b, 6g, h). *Flared slopes* are another concave features developed at the base of blocks (Table 1; Fig. 6h). They are parallel to the other directional features such as foliation and mineral alignment (Fig. 6h).

Weathering profiles are different from the other features listed above. The weathering can cause a layered structure from surface to subsurface (I to VI grade, Thomas 2004; Turkington 2004; Migoń 2006; Heidari et al. 2013; Miśćević and Vlastelica 2014). Grade VI represents soil horizon at the surface and heavy weathering, while grade I represents the fractured fresh rock (Thomas 2004). The typical weathering profile is only observed in quartz quarry and several road cuts (Table 1; Fig. 7a). The thicknesses of V and VI grades are increased in downdip direction (Fig. 7a). The boundary between the grades is not regular due to their irregular growth along the fractures (Fig. 7a). The weathering profile is thicker in the quarry than in the road cut.

Grus is weathered sediment derived from the upper part of the hill, transported in downdip direction and accumulated in lowland area among the hills (Table 1; Fig. 8b). The apparent thickness of quartz-rich sediment must be higher than 1–1.5.

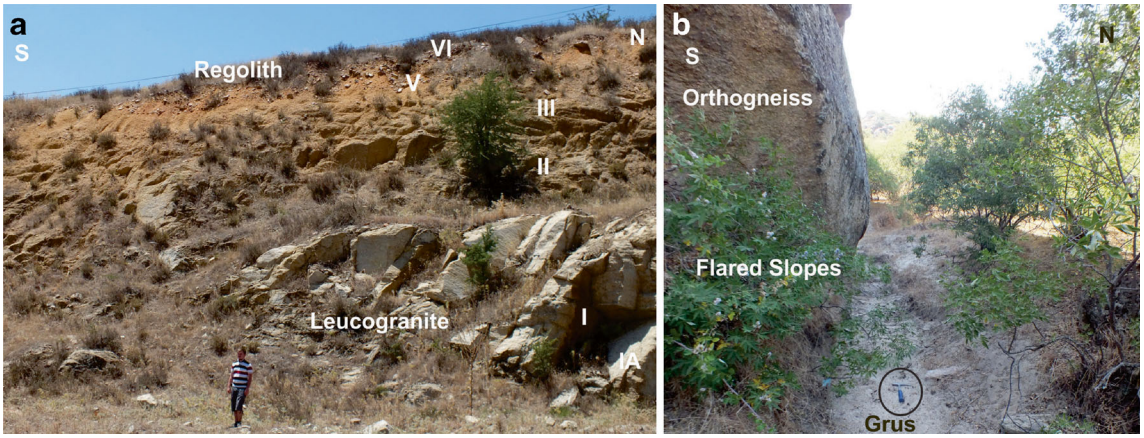

Fig. 7 **a** The deep weathering is rarely observed in the study area. The thickest one is observed in the quartz quarry in leucogranite in W Seykel District (*I* fresh rock, *II* slightly weathered, *III* moderately weathered, *V* completely weathered, *VI* residual soil; *man* for scale, 1.75 m). **b** The grus including gravelly sand has a sharp contact with the unweathered orthogneiss rock in N Hacıaliler District (*hammer* for scale, 33 cm)

Controlling factors for the development of gemorphological features

This section summarizes the controlling factors of geomorphological features observed within the study area. Fractures, exfoliation, climatic condition, rock strength, surface–underground water, biologic degradation, and subsurface weathering are the main controlling factors for the developments of geomorphological features in the granitoids (Twidale and Bourne 1975; Twidale 1986; Migoń 2004a, 2006; Twidale and Bourne 2008; Vidal Romani and Twidale 2010). Some of them are also important for the geomorphologic development and weathering of the Southern Submassif of Menderes Massif. These are listed below.

Structural alignments, pseudobedding (exfoliation cracks) Migoń (2006) has reported cross, longitudinal, and diagonal fractures in granite blocks, and weathering along those cracks caused pillar structure formation. The orthogneiss has three joint sets in the eastern part (no. 29, dip/dip direction, 75°/185°, 69°/239°, 65°/270°; foliation 30°/284°), and two joint sets in the northern part (no. 29, dip/dip direction 69°/172°, 76°/88°; foliation 17°/323°). Four joint sets and randomly distributed joints were measured in leucogranite (no. 22, dip/dip direction, 68°/12°, 67°/272°, 52°/58°, 20°/192°; foliation 25°/223°) (Fig. 8). N–S-directed joints are evaluated as a cross joint, and E–W-directed joints are evaluated as longitudinal fractures in blocks. The exhumation of orthogneiss and leucogranite causes exfoliation cracks parallel to foliation. The exhumation of the massif, emplacement of Lycian nappes, and compressional and extensional forces caused these fractures. The southern side of the study area is located within the boundary between the massif and cover units. Thus, the density of fractures in the southern part is higher than that in the northern part.

The crossing of fractures led to host rock fragmentation and pillar and block formation. Moreover, abundant fractures cause easy circulation of underground water, so weathering effects diffuse through the rock interior. Some researchers, mentioned in Table 1, proposed that subsurface weathering is important in the development of several distinct geomorphological features (flared slope, polygonal cracks, etc.). Similarly, the underground water percolates into the orthogneiss and leucogranite via using discontinuities. When the rock is exhumed, those weathered parts are stripped, and the hard-resistant unweathered parts remain.

Foliation, mineralogical contents The leucogranite consists of K-feldspar, plagioclase, quartz, muscovite, and biotite as primary minerals (Figs. 9a–c), whereas tourmaline, zircon, rutile, monazite, and opaques (e.g., magnetite) are accessory minerals (Bozkurt 2004). Quartz-tourmaline nodules reported by Bozkurt (2004) are also observed within the leucogranite. In addition, garnet minerals were determined under the microscope. The orthogneiss displays well-observed mylonitic foliation including parallel alignment of mica minerals (biotite and muscovite), quartz ribbons, and flattened feldspar porphyroclasts (Figs. 9d–f) and distinct NE-trending mineral lineation (Bozkurt 2004). Those bands can be easily followed during the field observations and petrographic analysis (Figs. 9e, f). Foliation of the orthogneiss is inclined to WNW. The flattened minerals are observed in leucogranite; however, they are not significant as in the case of orthogneiss. Mineral alignment of the leucogranite is inclined to SW. Wind and water (surface and underground water) are active along those features. Flared slopes and exfoliation cracks are parallel to foliation planes or mineral alignments in the study area. Red parts around the Fe-bearing minerals such as biotite exhibits the chemical weathering affects. Moreover, after the rapid weathering of less resistant minerals such as feldspar, durable

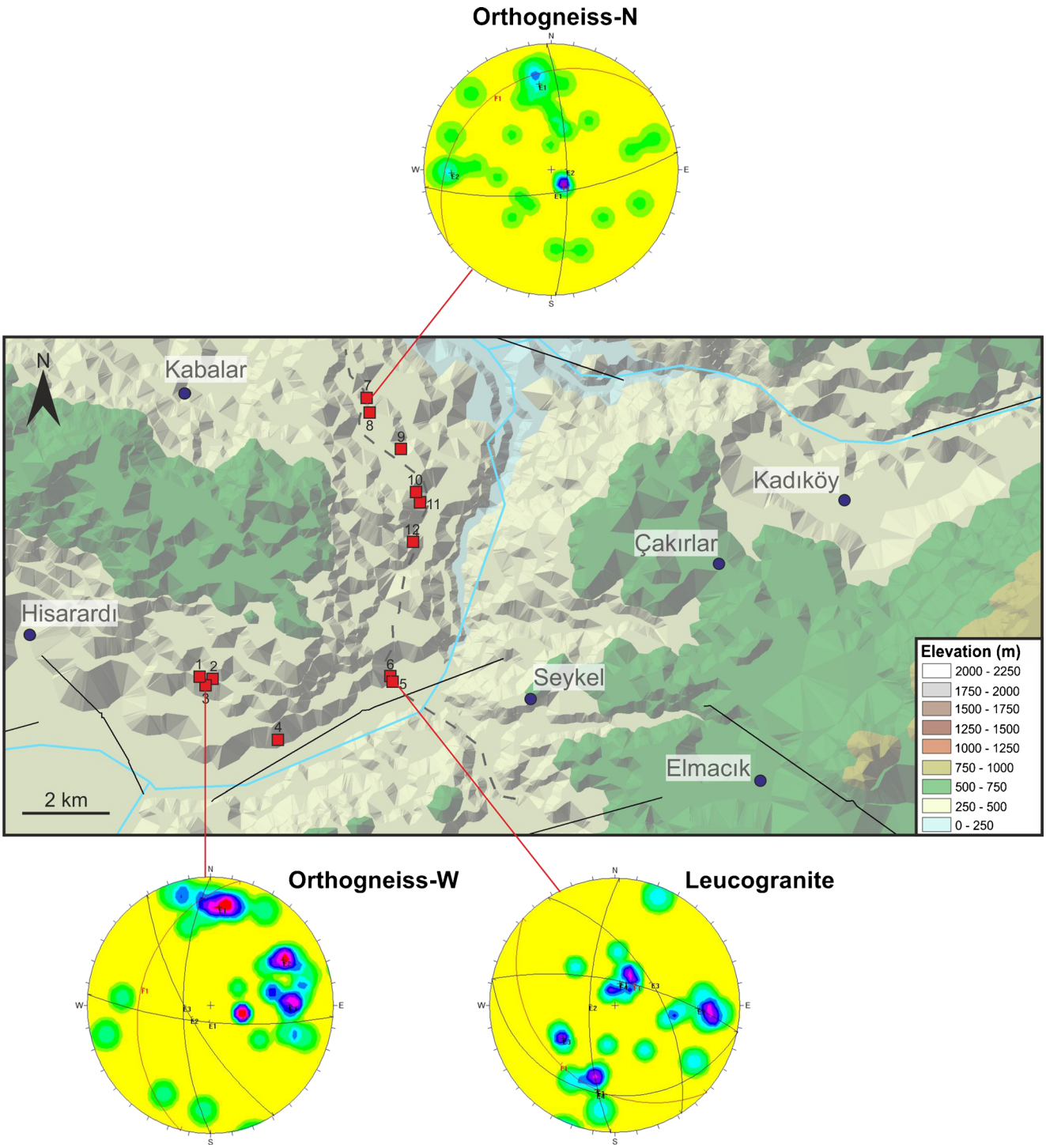

Fig. 8 DEM image of the detailed study area. Kinematic analyses of fractures measured from orthogneiss in N Hacıaliler District and W of the Memişler district. One location in S of Hacıaliler District has been chosen for fracture measurement in leucogranites

minerals like quartz start to be transported via slope, surface water, wind, and gravity and form grus (Fig. 7b).

Climatic condition Weathering caused by water, hydration, sapping, and halocasty are important processes in cavernous weathering (Strini et al. 2008; Twidale and Bourne 2008). When the rocks crop out, they will be under the effect of water attack, and this controls the weathering of rocks (Vidal Romani and Twidale 2010). Morever, tafoni enlargement is related to wind erosion, freezing, microclimatic conditions, and hydration (Twidale and Bourne 2008).

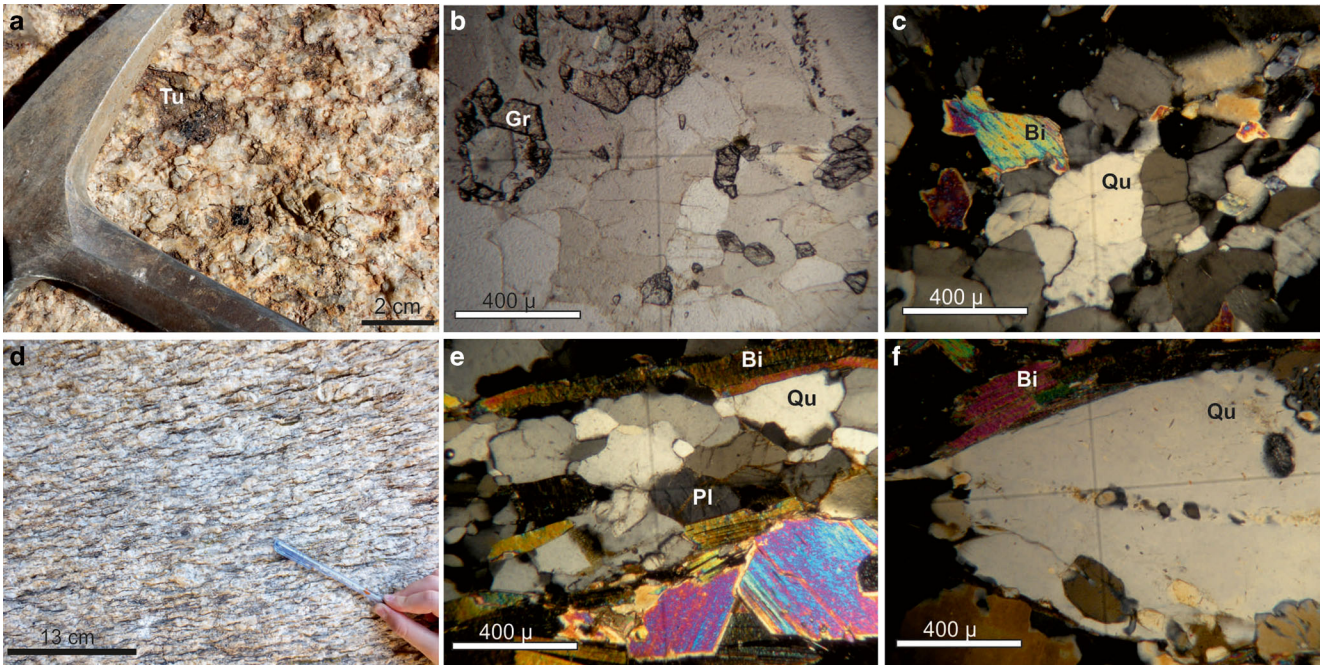

Fig. 9 **a** A close view of the metamorphosed leucogranites that include large glassy quartz, pink K-feldspar, and black tourmaline. **b** Euhedral–subhedral grant is also found in the thin section of leucogranites (under normal light). **c** Granat is surrounded by large quartz and biotite minerals (under polarized light) (*Tu* tourmaline, *Qu* quartz, *Bi* biotite, *Gr* granat, *Pl* plagioclase). **d** Gneissic banding observed in orthogneiss including gray-colored glassy quartz and white-colored large and elongated plagioclase. **e** The elongated biotite mineral, quartz, and plagioclase are found in this rock (under polarized light). **f** Sometimes, large quartz creates an augen gneiss view in the rock (under polarized light)

The leucogranite is exhumed after early Miocene (Bozkurt et al. 2015). Therefore, former and latter climatic conditions of exhumation are important. Akgün et al. (2007) reported that annual temperature varies (5.5–21.3 °C), as well as mean annual precipitation (1122–1520 mm) at Chattian and Aquitanian periods in western Anatolia. Mean annual temperature and precipitation were 1.1–20.8 °C and 1146–1322 mm, respectively, in the Early–Middle Serravallian–earliest Tortonian periods in Yatağan town, SW of the study area (Akgün et al. 2007). Lower precipitation was evaluated as 823 mm in the dry season during the middle–late Tortonian in this region (Akgün et al. 2007). Recently prevailing wind directions are S–E, N–E, and S–W in the study area (Haktanır et al. 2010; Ölgen and Gür 2011). The annual temperature of the Muğla region varies from −10.0 to 41.2 °C (56 years average; MGM 2013a, b); the annual average rainfall is 1130.5 mm (40 years average; MGM 2013a). These point out to the warmer climatic condition. Underground water percolation along the fracture is important in subsurface weathering. If recent climatic conditions were taken into consideration, wind weathering could have smoothened the sharp corner of the rock and promoted the spheroidal weathering and tafoni development and transportation of disintegrated rock fragments. The recent water leakages are particularly observed in the inner and outer parts of the rocks. Tafoni and honeycomb structures preserved inside into the tafoni have been developed within the rocks (Fig. 6e). The formation of weathering pits is also related to the movement of surface water on the rock surface (Fig. 6a).

Strength properties The Schmidt Hammer test is one of the in situ tests used for determining the strength of rocks during field study (Özbek and Gül 2011). The higher rebound values of this hammer point out the more resistant rock. Anisotropy of the rock due to bedding and foliation may affect the strength of rock (Ulusay and Gökçeoğlu 1997; Özbek 2009). Thus, the Schmidt hammer is applied perpendicular and parallel to the foliation. The average Schmidt hammer rebound value is 45.8 perpendicular to the mineral alignment in leucogranite, and 38.6 parallel to the alignment. The average Schmidt hammer rebound value is 42.5 perpendicular to the foliation in orthogneiss, and 29 parallel to the foliation. The strength of both rocks is lower in the direction parallel to the mineral alignment. Therefore, weathering of rock firstly develops parallel to the exfoliation then intrudes and extends through the interior of the rock. Anisotropy of the orthogneiss is larger than the leucogranite due to metamorphic texture development.

Discussion

The leucogranite and orthogneiss in the Southern Submassif of Menderes Massif in SW Turkey show some geomorphological

features that are typically reported in granitoids (Goudie 2004; Migoń 2006). Studies in the study area are mostly related to the general geological properties, deformation, and metamorphism history of the Menderes Massif (Bozkurt et al. 1995; Bozkurt and Satır 2000; Bozkurt and Oberhansli 2001; Whitney and Bozkurt 2002; Rimmele et al. 2003; Bozkurt 2004; Koralay et al. 2012; Bozkurt et al. 2015). These studies have not considered the geomorphological features of the Southern Submassif. Similarly, several studies about granitoids of Turkey have mainly focused on engineering properties of granitoids (Tuğrul and Zarif 1999; Ceryan et al. 2008; Dağdelenler et al. 2011; Kilic et al. 2014), whereas studies about their geomorphological features are limited (Erginal and Ertek 2008).

The inselbergs, domes, bornhardts, and tors are sharp hills surrounded by plain and macro landforms in granites (Ehlen 2004; Migoń 2004a, 2006; Twidale 2007). The domed bald hill and macro landforms of the study area (Figs. 1, 3, and 4) are surrounded by valleys. Exhumation of the massif led to its formation.

Pillar structures are pinnacle rockheads on low-lying host rock (Figs. 3, 4, and 5). The subsurface weathering during and after exhumation, surface weathering after exhumation, selective weathering along the fracture, and stripping of weathered units led to the formation of pillar structures, especially castellated-type pillar structures. Later surface weathering due to wind and water action may produce dome-topped pillar structures.

Migoń (2006) and Vidal Romani and Twidale (2010) emphasized that cross, longitudinal, and diagonal fractures or orthogonal structures in granite block increase the weathering effect. The orthogneiss has two and three joint sets, while leucogranite has four joint sets in the study area (Fig. 8). The southern part of the region has more discontinuity sets due to cover and core unit relations of the Southern Submassif. The exfoliation cracks act as another joint set at the upper part of units (Figs. 4 and 5a). Some joints are parallel to foliation of orthogneiss and mineral alignment of leucogranite, while some of them cut the foliation perpendicularly or obliquely. Those structures cause fragmentation of rocks and form a weakness zone for underground water action in subsurface environment. They led to the formation of attached and detached blocks (Figs. 3, 4, and 6f, g).

Mineral resistance and strength differentiation related to mineral alignment have significant effect on weathering. Migoń (2006) suggested that granular disintegration due to enlargement of mineral boundaries of granites promotes the weathering. The metamorphism of the studied units increases this effect. The metamorphism led to gneissic banding (Fig. 9), elongated and flattened alkali feldspar, quartz ribbons, and platy mica minerals (Bozkurt 2004). The resistances of those minerals are different. Mica minerals and feldspar can be easily eroded compared to the quartz.

Černa and Engel (2011) pointed out that the strength value of granite exposure is increased with depth based on the Schmidt hammer rebound values. The fracture density on surface and weathering led to low rebound values (Černa and Engel 2011). The granite has internal homogeneity in those applications, and the results are also valid for our study. However, the Schmidt hammer rebound values are variable in studied rock units due to mineral alignment and mineral content. The strength of orthogneiss is higher in perpendicular to the foliation than that parallel to the foliation. The leucogranite strength is relatively higher than that of orthogneiss in every direction because of mineral content and relatively low anisotropy. Thus, the weathering feature number of orthogneiss is relatively higher than that of leucogranite.

The fracture is splitted into several fragments of orthogneiss and leucogranite. Surface and underground water and wind action followed those weakness zones. They are especially acted at the crossing of joints, and the relatively low-resistant minerals start to weather. The weathering may cause a flared slope (Fig. 6h), spheroidal weathering (Figs. 5b and 6g, h), polygonal cracks (Figs. 5a and 6b), and weathering pits (Fig. 6a) on block surfaces (Fig. 7b). If the weathering affects the rock interior, cavernous type weathering such as tafoni (Figs. 5b and 6c–f) and honeycomb weathering (Fig. 6d) may develop.

In addition, Vidal Romani and Twidale (2010) reported that water caused the weathering of feldspar to clay, then led to the formation of quartz separation and grus. As a result of this process, similar quartz-rich grus filled the small valley of the study area (Fig. 7b).

Two stages of weathering are proposed for granitoid weathering, as the subsurface weathering (groundwater softening the main rock) and the stripping of regolith cover (Bourne and Twidale 2002; Vidal Romani and Twidale 2010). It is reported that the polygonal crack, boulder formation, pillar structure development, flared slopes, and grus formation are evaluated as a product of subsurface weathering by different researchers (Table 1). After the exposure of those structures, wind and surface water increase the weathering effect in the study area. Recent water traces in tafoni, honeycomb weathering, and weathering pit indicate the water effect.

All geomorphological landscapes listed above are determined in the Southern Submassif of Menderes Massif in SW Turkey, and they are observed in granitoids from different countries (USA, Ericson et al. 2005; Spain, Roqué et al. 2013; Portugal, Begonha and Sequeira Braga 2002; Ireland, Sweevers et al. 1995; Finland, Darmody et al. 2008; Central Europe, Migoń 1996; Iran, Heidari et al. 2013; Turkey, Erginal and Ertek 2008). Magma emplacement, tectonism, lithology, and fracture are proposed as main controlling factors for granitoid weathering (Migoń 2004a, 2006). In addition, tectonic and metamorphic history increases the

weathering effect in the study area. Especially foliation, mineral alignment, mineral content, strength differences of minerals, and development of various discontinuity sets are offered for the weathering in the study area. Combination of all those factors led to the formation of a good scene for possible geotourism activity. It is necessary to take urgent measures by local and central authorities for protecting those geomorphological features, or at least those peculiar ones.

Conclusions

The results obtained in this study are listed below.

- The study area includes orthogneiss and leucogranite that exhibit various geomorphological features of typical granitoid morphology. The larger features such as bald hill and pillar structures are well observed in the study area.
- The weathering pits, polygonal cracks, tafoni and honeycomb weathering, spheoridal weathering, flared slopes, and blocks have been determined in this study. The weathering profile and grus are also found.
- The tectonic alignments developed depending on the complex tectonic regime led to the fracturing of orthogneiss and leucogranite. Water follows these fractures in the subsurface. They initially control development of pillar structures, blocks, and boulders. The metamorphism of rocks caused foliation (i.e. gneissic banding and mineral alignment). Exhumation of these rocks formed exfoliation cracks. Strength differentiation of the foliated rocks and difference in mineral durability increase the weathering effect. Subsurface weathering led to formation of pillar structure, polygonal cracks, and flared slope. When weathered materials are stripped, they are exposed.
- Under the effect of previous controlling factors, wind and water have initially attacked the weakest part—sharp corner of the rocks under surface weathering. Firstly, round-edged spheroidal weathering is formed, and then tafoni and honeycomb weatherings are developed depending on the advancing of weathering to the rock body.

These special geomorphologic landscapes primarily need to be preserved by both locals and public administrations in order to prevent them from the mining companies and establish a geopark to this area.

References

Akgün F, Kayseri MS, Akkiraz MS (2007) Oligocene–Miocene period in Western and Central Anatolia (Turkey). Palaeogeogr Palaeoclimatol Palaeoecol 253:56–90

Begonha A, Sequeira Braga MA (2002) Weathering of the Oporto granite: geotechnical and physical properties. Catena 49:57–76

Bourne JA, Twidale CR (2002) Morphology and origin of three bornhardt inselbergs near Lake Johnston, Western Australia. J R Soc West Aust 85:83–102

Bozkurt E (2004) Granitoid rocks of the southern Menderes Massif (southwestern Turkey): field evidence for Tertiary magmatism in an extensional shear zone. International Journal Earth Science 93: 52–71

Bozkurt E, Winchester JA, Park RG (1995) Geochemistry and tectonic signifance of augen gneisses from the southern Menderes Massif (West Turkey). Geol Mag 132:287–301

Bozkurt E, Satır M (2000) New Rb-Sr geochronology from southern Menderes Massif (southwestern Turkey) and its tectonic signifance. Geol J 35:285–296

Bozkurt E, Oberhansli R (2001) Menderes Massif (western Turkey): structural, metamorphic and magmatic evolution—a synthesis. International Journal Earth Science 89:679–882

Bozkurt E, Ruffet G, Crowley QG (2015) Synorogenic Eocene leucogranite magmatism in the Southern Menderes Massif and its tectonic significance. 68th Geological Congress of Turkey, 06–10 Nisan/April 2015 MTA-Ankara-Turkey, 50–51

Campbell SW (1999) Chemical weathering associated with tafoni Atpapago Park Central Arizona. Earth Surf. Process. Landforms 24:271–278

Campbell EM, Twidale CR (1995) Lithologic and climatic convergence in granite morphology. Caderno Laboratory Xeolóxico de Laxe Coruña 20:381–403

Candan O, Dora Ö, Oberhansli R, Çetinkaplan M, Partzsch JH, Warkus FC, Dürr S (2001) Pan-African high-pressure metamorphism in the Precambrian basement of the Menderes Massif, western Anatolia, Turkey. International Journal Earth Science 89:793–811

Černa B, Engel Z (2011) Surface and sub-surface Schmidt hammer rebound value variation for a granite outcrop. Earth Surf. Process. Landforms 36:170–179. doi:10.1002/esp.2029

Ceryan S, Tudes S, Ceryan N (2008) A new quantitative weathering classification for igneous rocks. Environmental Geolology 55: 1319–1336

Dağdelenler G, Akcapinar-Sezer E, Gokceoglu C (2011) Some non-linear models to predict the weathering degrees of a granitic rock from physical and mechanical parameters. Expert Syst Appl 38:7476–7485

Darmody RG, Thorn CE, Seppälä M, Campbell SW, Li YK, Harbor J (2008) Age and weathering status of granite tors in Arctic Finland (~68° N). Geomorphology 94:10–23

Domínguez-Villar D, Jennings CE (2008) Multi-phase evolution of gnammas (weathering pits) in a Holocene deglacial granite landscape, Minnesota (USA). Earth Surf. Process. Landforms 33:165–177. doi:10.1002/esp.1532

Dora Ö, Candan O, Kaya O, Koralay OE, Dürr S (2001) Revision of the so-called "leptite-gniesses" in the Menderes Massif: a supracrustal metasedimentary origin. International Journal Earth Science 89(4): 836–851

Ehlen J (2004) Tor. In: Goudie AS (ed) Encyclopedia of geomorphology. London, Routledge, pp. 1054–1056

Erginal AE, Ertek A (2008) Some geomorphological features of the Orhaneli Pluton: implications for denudation history. Mineral Research Exploration Bulletin 137:61–72

Ericson K, Migon P, Olvmo M (2005) Fractures and drainage in the granite mountainous area a study from Sierra Nevada, USA. Geomorphology 64:97–116

Görür N, Şengör AMC, Sakınç M, Tüysüz O, Akkük R, Yiğitbaş E, Oktay FY, Barka AA, Sarıca N, Ecevitoğlu B, Demirbağ E, Ersoy Ş, Algan O, Güneysu C, Akyol A (1995) Rift formation in the Gökova region, southwest Anatolia: implications for the opening of the Aegean Sea. Geol Mag 132:637–650

Goudie AS (2004) Encyclopedia of geomorphology. Goudie AS (Ed). Routledge, London

Gürer ÖF, Yılmaz Y (2002) Geology of the Ören and surrounding regions, SW Turkey. Turkish Journal of Earth Science 11:2–18

Haktanır K, Sözüdoğru-Ok S, Karaca A, Arcak S, Çimen F, Topcuoğlu B, Türkmen C, Yıldız H (2010) Muğla-Yatağan Termik Santralı Emisyonlarının Etkisinde Kalan Tarım ve Orman Topraklarının Kirlilik Veri Tabanının Oluşturulması Ve Emisyonların Vejetasyona Etkilerinin Araştırılması. Ankara Üniversitesi Çevre Bilimleri Dergisi 2:13–30 (in Turkish with English abstract)

Heidari M, Momeni AA, Naseri F (2013) New weathering classifications for granitic rocks based on geomechanical parameters. Eng Geol 166:65–73

Kilic R, Ulamis K, Yurdakul M, Kadioglu YK (2014) The alteration degree of the metacrystalline rocks based on UAI, Bolu (Turkey). Bulletin Engineering Geology Environment 73:193–201

Koralay OE, Candan O, Chen F, Akal C, Oberhansli R, Satır M, Dora OÖ (2012) Pan-African magmatism in the Menderes Massif: geochronological data from leuco tourmaline orthogneisses in western Turkey. International Journal Earth Science 101:2055–2081

MGM (2013a) http://www.mgm.gov.tr/veridegerlendirme/il-ve-ilceler-istatistik.aspx?m=MUGLA (Access date: 25.05.2013)

MGM (2013b) http://www.mgm.gov.tr/veridegerlendirme/yillik-toplam-yagis-verileri.aspx?m=MUGLA (Access date: 25.05.2013)

Migoń P (1996) Evolution of granite landscapes in the Sudetes (Central Europe): some problems of interpretation. Proc Geol Assoc 107:25–37

Migoń P (2004a) Structural control in the evolution of granite landscape. Acta Universitatis Carolinae, Geographica 1:19–32

Migoń P (2004b) Granite geomorphology. In: Goudie AS (ed) Encyclopedia of geomorphology. Routledge, London, pp. 490–493

Migoń P (2006) Geomorphological landscapes of the world. In: Migoń P (ed) Granite landscapes of the world. Oxford University Press Inc., New York, p. 416

Migoń P, Vieira G (2014) Granite geomorphology and its geological controls, Serra da Estrela, Portugal. Geomorphology 226:1–14

Mišćević P, Vlastelica G (2014) Impact of weathering on slope stability in soft rock mass. J Rock Mech Geotech Eng 6-3:240–250

Nicholson DT (2004) Spheroidal weathering. In: Goudie AS (ed) Encyclopedia of geomorphology. Routledge, London, p. 992

Okay Aİ (2001) Stratigraphic and metamorphic inversions in the central Menderes Massif: a new structural model. International Journal Earth Science 89:709–727

Ölgen MK, Gür F (2011) Geographical distribution of heavy metal pollution in lichens (Xanthoriaparietina) in the vicinity of Yatağan coal fired power plant. Turkish Journal of Geography 57:43–54 (in Turkish with English abstract)

Özbek A (2009) Variation of Schmidt hammer values with imbrication direction in clastic sedimentary rocks. International Journal of Rock Mechanics Minining Science 46:548–554

Özbek A, Gül M (2011) Variation of Schmidt hammer rebound values depending on bed thickness and discontinuity surfaces. Sci Res Essays 6-10:2201–2211

Özer S, Sözbilir H, Özkar İ, Toker V, Sarı B (2001) Stratigraphy of Upper Cretaceous-Paleogene sequences in the southern and eastern Menderes Massif (western Turkey). International Journal Earth Science 89:852–866

Rimmele G, Jolivet L, Oberhansli R, Goffe B (2003) Deformation history of the high-pressure Lycian Nappes and implications for tectonic evolution of SW Turkey. Tectonics 22:1007–1027

Robertson AHF (2000) Mesozoic-Tertiary tectonic-sedimentary evolution of a south Tetyhan oceanic basin and its margins in southern Turkey. In: Tectonics and magmatism in Turkey and the surrounding area, Bozkurt E, Winchester JA, Piper JDA, (Eds.). Geological Society, London, Special Publications 173: 353–384

Roqué C, Zarroca M, Linares R (2013) Subsurface initiation of tafoni in granite terrains—geophysical evidence from NE Spain: geomorphological implications. Geomorphology 196:94–105

Şenel H (1997) Inversion of gravity anomaly of Büyük Menderes faults. Journal of Kocaeli University 4:66–72

Şengör AMC, Yılmaz Y (1981) Tethyan evolution of Turkey: a plate tectonic approach. Tectonophysics 75:181–241

Şengör AMC, Satır M, Akkök R (1984) Timing of tectonic events in the Menderes Massif, western Turkey: implications for tectonic evolution and evidence for Pan-African basement in Turkey. Tectonics 3: 693–707

Strini A, Guglielmin M, Hall K (2008) Tafoni development in a cryotic environment: an example from Northern Victoria Land, Antartica. Earth Surf. Process. Landforms 33:1502–1519. doi:10.1002/esp.1620

Sweevers H, Peeters A, Van Grieken R (1995) Weathering of Leinster granite under ambient atmospheric conditions. Sci Total Environ 167:73–85

Thomas MF (2004) Deep weathering. In: Goudie AS (ed) Encyclopedia of geomorphology. Routledge, London, pp. 228–233

Tuğrul A, Zarif IH (1999) Correlation of mineralogical and textural characteristics with engineering properties of selected granitic rocks from Turkey. Eng Geol 51-4:303–317

Turkington A (2004) Mechanical weathering. In: Goudie AS (ed) Encyclopedia of geomorphology. Routledge, London, p 657–659

Turkington AV, Phillips JD (2004) Cavernous weathering, dynamical instability and self-organization. Earth Surf Process Landforms 29: 665–675

Twidale CR (1986) Granite landform evolution: factors and implications. Geol Rundsch 75-3:769–779

Twidale CR (1995) Bornhardts, boulders, inselbergs. Cadernos Laboratory Xeolóxico de Laxe Coruña 20:347–380

Twidale CR (1997) Some recently developed landforms: climatic implications. Geomorphology 19:349–365

Twidale CR (2002) The two-stage concept of landform and landscape development involving etching: origin, development and implications of an idea. Earth Sci Rev 57:37–74

Twidale CR (2007) Bornhardts and associated fracture patterns. Rev Asoc Geol Argent 62-1:139–153

Twidale CR, Bourne JA (1975) The subsurface initiation of some minor granite landforms. Journal of the Geological Society of Australia: An International Geoscience Journal of the Geological Society of Australia 22-4:477–484. doi:10.1080/00167617508728912

Twidale CR, Bourne JA (1998) Origin and age of bornhardts, southwest Western Australia. Australian Journal of the Earth Science 45:903–914

Twidale CR, Bourne JA (2003) Origin and inversion of fluting in granitic rocks. Australian Journal of the Earth Science 50:543–552

Twidale CR, Bourne JA (2008) Caves in granitic rocks: types, terminology and origins, Cadernos Lab. Xeolóxico de LaxeCoruña 33:35–57

Ulusay R, Gökçeoğlu C (1997) The modified block punch index test. Canadian Geotechical Journal 34:991–1001

Vidal Romani JR, Twidale CR (2010) Structural or climatic control in granite landforms? The development of sheet structure, foliation, boudinage, and related features. Cadernos Laboratory Xeolóxico de Laxe Coruña 35:189–208

Whitney DL, Bozkurt E (2002) Metamorphic history of the southern Menderes Massif, western Turkey. Geological Society of American Bulletin 114:829–838